Surface-Induced Polymerization of Actin

Anne Renault,* Pierre-François Lenne,* Cécile Zakri,* Achod Aradian,§ Catherine Vénien-Bryan,# and François Amblard§

*Laboratoire de Spectrométrie Physique, Centre National de la Recherche Scientifique, UMR-5588, BP87, 38402 St Martin d'Heres; #Institut de Biologie Structurale Jean-Pierre Ebel, Commissariat à l'Energie Atomique et Centre National de la Recherche Scientifique, 38027 Grenoble Cédex 1; and §Laboratoire de Physiologie, Ecole Supérieure de Physique et Chimie Industrielle et Centre National de la Recherche Scientifique, UMR-7637-Neurobiologie, 75231 Paris Cedex 05, France

ABSTRACT Living cells contain a very large amount of membrane surface area, which potentially influences the direction, the kinetics, and the localization of biochemical reactions. This paper quantitatively evaluates the possibility that a lipid monolayer can adsorb actin from a nonpolymerizing solution, induce its polymerization, and form a 2D network of individual actin filaments, in conditions that forbid bulk polymerization. G- and F-actin solutions were studied beneath saturated Langmuir monolayers containing phosphatidylcholine (PC, neutral) and stearylamine (SA, a positively charged surfactant) at PC:SA = 3:1 molar ratio. Ellipsometry, tensiometry, shear elastic measurements, electron microscopy, and dark-field light microscopy were used to characterize the adsorption kinetics and the interfacial polymerization of actin. In all cases studied, actin follows a monoexponential reaction-limited adsorption with similar time constants ($\sim 10^3$ s). At a longer time scale the shear elasticity of the monomeric actin adsorbate increases only in the presence of lipids, to a 2D shear elastic modulus of $\mu \approx 30$ mN/m, indicating the formation of a structure coupled to the monolayer. Electron microscopy shows the formation of a 2D network of actin filaments at the PC:SA surface, and several arguments strongly suggest that this network is indeed causing the observed elasticity. Adsorption of F-actin to PC:SA leads more quickly to a silghtly more rigid interface with a modulus of $\mu \approx 50$ mN/m.

INTRODUCTION

Actin is the major constituent of muscle cells, but it is also expressed in the cytoplasm of all eukaryotic cells, where it plays a central role in numerous cellular functions such as cell motility, cytokinesis, and phagocytosis (Pollard, 1990; Kabsch and Vandekerckhove, 1992). Since actin purification procedures have been available, actin has been studied for its biochemical and physical properties. In vivo, monomeric actin, also called G-actin, can reversibly polymerize into microfilaments called F-actin, under the control of several intricate and distinct regulatory pathways that have been studied extensively (Carlier, 1991; Sheterline and Sparrow, 1994). In vitro, G-actin is classically induced to polymerize by salts such as KCl and $MgCl_2$ or polyamines (Oriol-Audit, 1978; Grant and Oriol-Audit, 1983), and the resulting F-actin solutions have been investigated by numerous groups for their macroscopic (Janmey, 1991; Maggs, 1997) and microscopic viscoelastic properties (Ziemann et al., 1994; Amblard et al., 1996; Schnurr et al., 1997).

Motivated by the elucidation of its structure, efforts have been made to crystallize the actin monomer, and various strategies have been used. The crystal structure of the monomer is not yet available, although cocrystals between F-actin and different actin-binding proteins have been made and resolved successfully, such as those with profilin, DNAse I, and gelsolin (Mannherz, 1992, and Pollard et al., 1994, for reviews). On the one hand, in 3D, under well-defined ionic conditions with polycationic molecules or multivalent cations, pure actin assembles into microfilaments that form superstructures such as elongated microcrystals, tubules, or stacks of parallel filament sheets (see Taylor and Taylor, 1992, for a review). On the other hand, solutions of filaments were shown to adsorb to positively charged 2D substrates by electrostatic interaction and assemble into flat paracrystalline filament arrays, from which low-resolution structural information was obtained (Rioux and Gicquaud, 1985; Ward et al., 1990; Taylor and Taylor, 1992, and references therein). Because actin has a low pI ($\sim$5.5), its electrostatic adsorption can be obtained at neutral pH on polyamine surfaces, mixtures of neutral and basic lipids (Rioux and Gicquaud, 1985; Laliberté and Gicquaud, 1988; Ward et al., 1990), or with basic surfactants (Taylor and Taylor, 1992). In most studies, the buffer conditions have been such that bulk polymerization in the solution generally precedes the surface adsorption of polymers and paracrystal formation, and not much attention has been paid to the possible scenario of surface-induced polymerization from a nonpolymerizing monomer solution. One report shows surface-induced polymerization by positively charged liposomes, leading to paracrystal formation, but single filaments were not observed (Laliberté and Gicquaud, 1988).

Because the organization of biological membranes is a central question in cell biology, several studies have been devoted to the lateral behavior of membrane proteins and to lipid/lipid and lipid/protein interactions (Jacobson et al., 1995). In this context, the 2D crystallization of soluble

Received for publication 2 April 1998 and in final form 25 November 1998.

Address reprint requests to Dr. François Amblard, Laboratoire de Physico-Chimie, Institut Curie, 11 rue Pierre et Marie Curie, 75005 Paris, France. Tel.: 33-1-42346795; Fax: 33-1-42346795; E-mail: francois.amblard@curie.fr.

0006-3495/99/03/1580/11 $2.00

proteins by means of a lipid monolayer has been studied by powerful structural methods such as grazing incidence x-ray diffraction (Haas et al., 1995; Lenne, 1998), and electron cryomicroscopy (Henderson et al., 1990). In addition, the measurement of the surface viscoelasticity has been recently combined with ellipsometry (Vénien-Bryan et al., 1998). Nevertheless, most proteins studied so far in 2D do not assemble into linear polymers, but rather into 2D arrays, and the possibility of polymerization from a solution of 2D confined monomers has not been investigated.

The aim of the present work is to investigate the process by which a positively charged lipid monolayer deposited at the air/buffer interface could serve as a template for the polymerization of monomeric actin into single filaments. We wish to establish a reproducible set of qualitative and quantitative observations that demonstrates surface-induced polymerization of actin and describes some of its kinetic, mechanical, and ultrastructural aspects. Following initial work (Renault et al., 1997), the adsorption kinetics and the process of surface polymerization are studied by ellipsometry, tensiometry, surface rheology, and dark-field light microscopy. The ultrastructure of single 2D-formed polymers is approached by electron microscopy. The role of the surface lipids and the dimensionality of the polymerization process are evaluated by contrasting experimental conditions: G- or F-actin at a bare air/water interface or under a lipid monolayer.

MATERIALS AND METHODS

Lipid and actin biochemistry

Egg phosphatidylcholine (PC, Sigma catalog no. P-5763) and stearylamine (SA, Sigma catalog no. S-9273) were kept in hexane/ethanol solution (9:1) at −20°C. The working solutions were prepared in chloroform or in hexane/ethanol at a final lipid concentration of 6×10^{-4} M. Positively charged amphiphiles (SA) were mixed with PC as the neutral lipid, at a final molar ratio of PC:SA of 3:1. Following the classical method of Pardee and Spudich (1982), actin acetone powder was prepared from chicken breast muscles and stored at −80°C. Actin was then extracted through two or three cycles of polymerization-depolymerization. High-salt washes were performed with 0.65 M KCl for 30 min, and filaments were depolymerized by rapid overnight dialysis in G-buffer (5 mM Tris-HCl, pH 7.4, 0.2 mM Na-ATP, 0.5 mM β-mercaptoethanol, 0.2 mM $CaCl_2$, and 0.01% NaN_3), followed by ultracentrifugation. The purity was assessed by electrophoresis, using Coomassie staining-overloaded polyacrylamide gels, and by MALDI-TOF mass spectrometry (Perseptive, Framingham, MA). Highly purified G-actin solution was stored at −80°C. Samples were prepared by diluting concentrated actin in nonpolymerizing buffer (G-buffer) or polymerizing buffer (F-buffer), that is, G-buffer supplemented with 100 mM KCl, 2 mM $MgCl_2$, and 0.5 mM Na-ATP.

Ellipsometry, surface tension

The ellipsometric measurements were carried out with a conventional null ellipsometer using a He-Ne laser operating at 632.8 nm (Berge and Renault, 1993). The variation of the ellipsometric angle is a relevant probe for changes occurring at the interface. Ellipsometric angle (Δ) and surface pressure were recorded simultaneously. The surface pressure was measured with a Wilhelmy balance. The sample cell is made from Teflon and has a volume of 8 ml. The protein is injected into the subphase, and the buffer is then coated by the lipid monolayer. All the experiments were carried out at room temperature. Initial time points of all graphs ($t = 0$) correspond to the first possible measurements, once the surface is stable, i.e., a few minutes after mixing.

Shear elastic constant

The rheometer set-up uses the action of a very light float (32 mg), which applies a rotational strain to the monolayer through a magnetic torque (with a pair of Helmholtz coils and a small magnetized pin deposited in the float). This set-up and the procedure for data analysis have been described previously (Vénien-Bryan et al., 1998; Zakri-Delplanque, 1997). Briefly, at the center of a 48-mm-diameter Teflon trough, a 10-mm-diameter paraffin-coated aluminum disc floats at the air/water interface, surrounded by the monolayer, whose rigidity is measured. The subphase is 5 mm deep. The float carries a small magnet and is kept centered by a permanent field, $B_0 = 6 \times 10^{-5}$ T, parallel to the Earth's field and created by a little solenoid located just above the float. Sensitive angular detection of the float rotation is achieved by using a mirror fixed on the magnet to reflect a laser beam onto a differential photodiode. A sinusoidal torque excitation is applied to the float in the 0.01–100 Hz frequency range, by an oscillating field perpendicular to the permanent solenoid field. The latter field acts as a restoring torque equivalent to a monolayer with a rigidity of 0.16 mN/m. This number set the sensitivity limit of this rheometer. The device behaves like a simple harmonic oscillator. The angular response is measured in amplitude and phase and is considered to reflect directly the rotational strain of the monolayer (see the Discussion). The data presented here only include the values of the shear elastic constant, μ (mN/m), measured at 5 Hz. Initial time points of all graphs ($t = 0$) correspond to the first possible measurements, once the magnetic float is centered and stable, i.e., a few minutes after mixing.

Electron microscopy

At the end of the experiments, i.e., after 20 h, plain carbon-coated electron microscope grids were placed on top of the crystallization trough, withdrawn after a few minutes of adsorption, and negatively stained with 2% (w/v) uranyl acetate for 30 s. Negatively stained specimens were examined in a Philips CM200 electron microscope operating at 200 kV. Micrographs were recorded on Kodak SO 163 film under low dose conditions and at a nominal magnification of 27,500×. For some experiments, the subphase was mildly stirred by a slowly rotating magnetic bar lying on the bottom of the trough, with dimensions and an angular velocity such that it does not disrupt the surface.

Dark-field light microscopy

The air/water interface was imaged with an inverted microscope (IX; Olympus, Japan) equipped with a 100-W halogen lamp and commercially available dry optics: a dark-field condenser (U-DCD) and a 60× UPlFL objective. A ULL760 intensified CCD (Lhesa, Cergy Pontoise, France) was used for video-rate imaging of actin filaments at the interface.

RESULTS

G-Actin at the air/buffer interface

In a first set of experiments, the surface properties of the air interface of G- and F-actin solutions are characterized by ellipsometry and shear elastic measurements. The time course of the ellipsometric angle for the adsorption of actin (25 μg/ml, i.e., 0.6 μM) in G-buffer on the air/water interface clearly shows two distinct kinetic phases (Fig. 1). Based on five independent experiments at short times (<7000 s), the adsorption fits with an exponential behavior

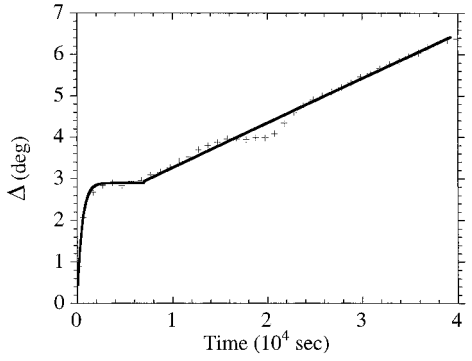

FIGURE 1 Ellipsometric angle Δ versus time, for 25 μg/ml actin in G-buffer at the bare air/water interface. +, Data points; ——, fit (see text).

with an asymptotic angle of $\Delta_{max} = 2.9$ (±0.4 deg) and a time constant of $\tau = 0.50 \pm 0.02 \times 10^3$ s (Table 1). At longer times (>7000 s), a linear increase of the ellipsometric angle dominates the exponential with a slope of $9.3 \pm 0.1 \times 10^3$ deg · s^{-1}.

The first of these two kinetic phases of the ellipsometric angle probably reflects the adsorption of the G-actin at the interface. The exponential kinetics is in agreement with a first-order process, and its asymptotic value suggests that the adsorbed layer is not dense. By changing the initial actin concentration to 9 μg/ml (reduction by a factor of 3), the fitted time τ is multiplied by 3, and Δ_{max} is lower because of a decrease in the actin surface density (data not shown). Throughout these experiments, the lateral pressure is constant and close to zero, and the viscoelastic response cannot be distinguished from that of water, meaning that the modulus is less than 0.15 mN · m^{-1}.

F-Actin at the air/buffer interface

Actin is then polymerized at 25 μg/ml in an F-buffer subphase containing 100 mM KCl and 1 mM $MgCl_2$. The ellipsometric response (Fig. 2 *a*) can be fitted with an exponential behavior superimposed on a linear increase that dominates at long times. For five independent experiments, the fitted time constants and asymptotic values of the exponential behavior are similar within the fit errors, with $\Delta_{max} = 8.5 \pm 0.5$ deg, and $\tau = 1.12 \pm 0.04 \times 10^3$ s,

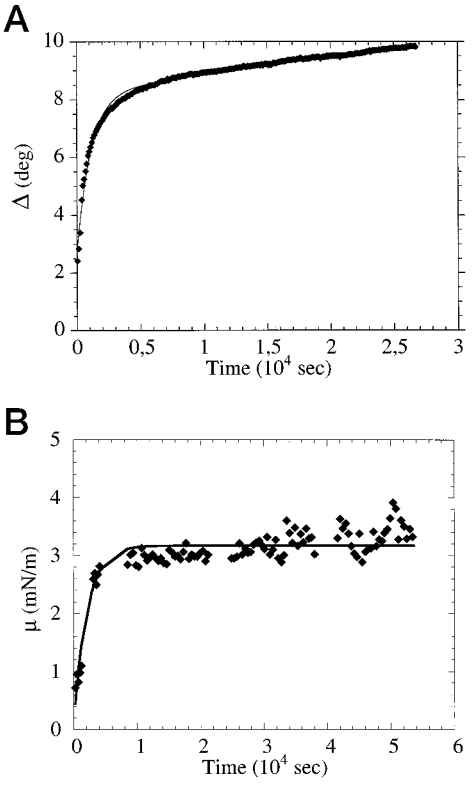

FIGURE 2 (*a*) Ellipsometric angle Δ versus time, for 25 μg/ml actin in F-buffer at the bare air/water interface. (*b*) Shear elastic constant μ versus time, for 25 μg/ml F-actin in F-buffer at the bare air/water interface. ♦, Data points; ——, fit (see text).

whereas the long time slope is ~15×10^3 deg · s^{-1}. As for G-actin, a lower actin concentration (9 μg/ml) gives similar results, i.e., the fitted value of τ is inversely proportional to the bulk concentration (data not shown).

The time evolution of the surface elastic constant μ (Fig. 2 *b*) for two independent experiments shows a plateau value $\mu_{max} = 3.0 \pm 0.3$ mN · m^{-1}, with an interexperiment deviation on the same order of magnitude as the fit error. The typical time necessary to reach this plateau is estimated from an exponential fit to be on the order of $\tau_{el} = 2.1 \times 10^3$ s. Adsorption and rigidification processes can thus be considered to overlap in time. Surface tension measurements display an increase in the lateral pressure toward a plateau

TABLE 1 Kinetic constants and amplitude extracted from ellipsometric and elasticity measurements

	G-buffer/air	G-buffer/*lipid*	F-buffer/air	F-buffer/*lipid*
Δ_{max} (deg)	2.9 ± 0.4	5.4 + *8.6* ± 0.8	8.5 ± 0.5	10.4 + *8.6* ± 1.5
τ (×10^3 s)	0.50 ± 0.02	1.83 ± 0.04	1.12 ± 0.04	3.9 ± 0.2
μ_{max} (mN/m)	<1	30 ± 5	3.0 ± 0.3	49 ± 5
τ_{el} (× 10^3 s)	NA	80	2.1*	2.0*

Δ_{max} (deg) is the asymptotic amplitude of the ellipsometric response, and τ (s) the characteristic time of its increase. Δ_{max} is given as the sum of the protein signal and the lipid offset (~8.6, in italics), together with the error on the determination of the fitted value. The deviation of the fitted values for five independent experiments was less than the fit errors given. μ (mN/m) is the asymptotic value of the surface elastic modulus, and τ_{el} (s) is the characteristic time of its increase, as estimated from exponential fits (see text). μ is the mean of the fits of two or three experiments, followed by the interexperiment deviation of the fitted values.

*These time constants are typical values, but no meaningful deviations are given because of the time required to stabilize the rotating float.

value of ~15 mN · m^{-1}, within the same typical time (data not shown). The shear elasticity of the F-actin measured at the air/water interface could be due to the coupling between the surface and the 3D filament network in the bulk, and/or to the surface structure itself, as suggested by the increase in lateral pressure.

The above exponential fits (Figs. 1 and 2) were computed with time offsets that are not discussed here, because they are essentially due to technical factors: 1) F-actin samples are prepared and induced to polymerize before they are loaded into the trough. 2) The mechanical stabilization of the sample and float required for shear elasticity measurements takes several minutes. 3) The initial time points $t = 0$ on all figures correspond to the time of the first measurement. The same remarks apply to Figs. 3 and 4.

Actin under lipid monolayers

All experiments are realized at a lateral pressure corresponding to surface saturation, slightly below the collapse pressure of the lipid monolayers: $\Pi = 30 \pm 5$ mN · m^{-1}. Saturation is obtained by the successive addition of lipid solution. Several studies have shown that the mixture of a zwitterionic lipid (PC) and a very poorly soluble, positively charged amphiphile (SA) behaves as an adequate monolayer substrate for the adsorption of F-actin (see Taylor and Taylor, 1992, for review). The classical PC:SA mixture (of a 3:1 molar ratio) is used here. The viscoelastic response shows that the monolayer alone is in fluid phase at room temperature, which is a prerequisite for our experiments. Indeed, the elastic response could not be distinguished from that of water, indicating that the modulus is less than ~0.15 mN · m^{-1}. The ellipsometric angle of the bare lipid monolayer very reproducibly yields a $\Delta_{max} = 7.6 \pm 0.4°$ at saturation.

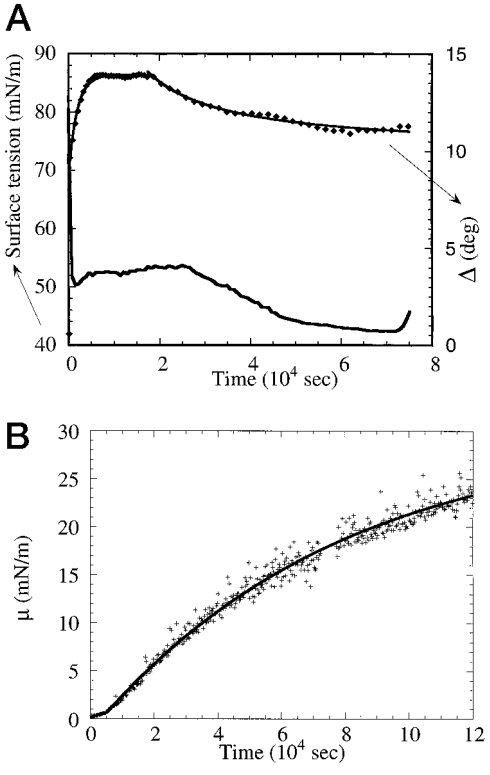

FIGURE 3 Actin in "nonpolymerizing" G-buffer under the PC:SA lipid monolayer, at 25 μg/ml. (*a*) Ellipsometric angle Δ versus time with raw data (♦) and fit (——), and surface tension versus time (raw data: ——). (*b*) Shear elastic constant μ versus time, with data points (+) and fit (——) (see text).

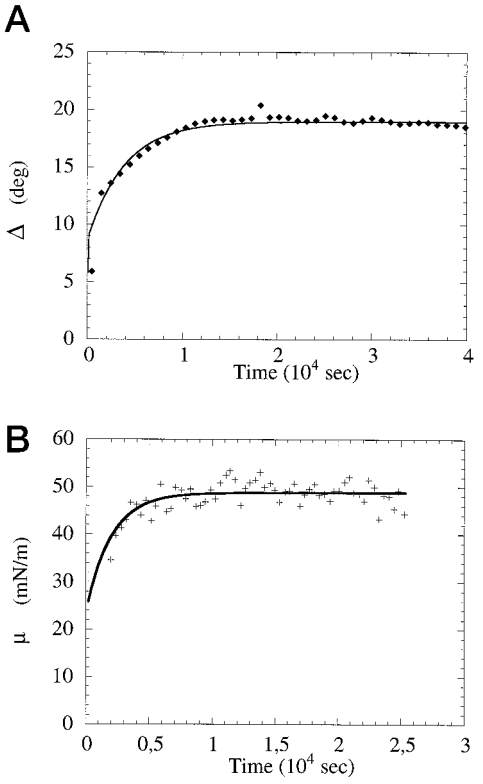

FIGURE 4 Actin in "polymerization" F-buffer under the PC:SA lipid monolayer, at 22 μg/ml. (*a*) Ellipsometric angle Δ versus time, with raw data (♦) and fit (——). (*b*) Shear elastic constant μ versus time, with raw data (+) and fit (——).

Actin in G-buffer under lipid monolayers

G-actin is injected into a G-buffer subphase at a final concentration of 25 μg/ml. Lipids are then deposited to form a stable monolayer at the surface. The time course of the ellipsometric angle for the adsorption of G-actin under the lipid monolayer clearly shows two distinct kinetic phases (Fig. 3 *a*). At short times ($t < 17.5 \times 10^3$ s) the adsorption follows an exponential behavior: $\Delta = \Delta_0 + \Delta_{max}(1 - e^{-(t/\tau)})$ with $\Delta_0 = 8.6 \pm 0.5$ deg, $\Delta_{max} = 5.4 \pm 0.8$ deg, and $\tau = 1.83 \pm 0.04 \times 10^3$ s. The offset value Δ_0 is a free parameter of the fit corresponding to the angle of the lipid monolayer alone. These fitted values were the same for two independent experiments. The fitted value of Δ_0 is close to the value determined above for bare lipids (7.6 deg). At long times ($>17.5 \times 10^3$ s), the decrease in the ellipsometric angle best fits with a hyperbolic time depen-

dence as $\Delta(t) = \Delta' + \tau' \cdot t^{-1}$, with $\Delta' = 10.1$ deg and $\tau' = 70 \times 10^3$ s · deg. The time evolution of the surface tension (Fig. 3 *a*) also follows that of the ellipsometric angle, with two clearly distinct kinetic processes.

The shear elastic constant rises with time (Fig. 3 *b*). An exponential fit yields a plateau shear elasticity of $\mu_{max} = 30$ mN/m with a deviation of 5 mN/m for the three experiments realized. The typical exponential time, τ_{el}, was 8×10^4 s. This increase in τ_{el} is due to the specific interaction between G-actin and the lipid monolayer, because either monolayer lipids or G-actin alone give no detectable elastic response.

F-Actin under lipid monolayers

Monomeric actin was injected into an F-buffer subphase at 22 μg/ml and then covered by a saturated lipid monolayer. The time course of the ellipsometric angle for the adsorption again follows an exponential behavior (Fig. 4 *a*): $\Delta = \Delta_0 + \Delta_{max}(1 - e^{-(t/\tau)})$, with $\Delta_0 = 8.6 \pm 0.5$ deg, $\Delta_{max} = 10.4 \pm 1.5$ deg, and $\tau = 3.9 \pm 0.2 \times 10^3$ s. The offset value Δ_0 is a free parameter of the fit that corresponds to the bare lipid monolayer angle previously determined and is close to the value measured in G-actin experiments (Table 1). Nevertheless, the adsorption kinetics of G- and F-actin under lipids show some differences (Figs. 3 *a* and 4 *a*): 1) the characteristic time τ is twice as long for F-actin, 2) there is no hyperbolic decrease at long times for F-actin, and 3) the asymptotic value of Δ is twice that of G-actin adsorption before its hyperbolic decrease.

The shear elastic constant (Fig. 4 *b*) reaches a plateau elasticity $\mu_{max} = 49 \pm 5$ mN/m for two independent experiments. The typical time of that process is $\tau_{el} = 2.0 \times 10^3$ s. The magnitude of the shear elasticity increase is much larger than that of F-actin at the air-water interface. This is consistent with the idea that lipids induce a strong coupling between the surface and the bulk F-actin solution. Under lipids, the higher elastic constant obtained over the F-buffer subphase compared to that with the G-buffer can also be explained by this coupling with the bulk. The characteristic time τ_{el} is approximately half the characteristic time of the ellipsometric angle (4000 s). This kinetic difference indicates that the increase in surface shear elasticity is not due solely to F-actin adsorption, but also to coupling with the bulk subphase. Indeed, bulk coupling is achieved as soon as filaments "stick" to the monolayer at any contact point, whereas the ellipsometric angle still increases when filaments extend their contact length with the surface.

Electron microscopy observations

In nonpolymerizing conditions, i.e., without KCl and $MgCl_2$, electron micrographs of the bare air/buffer interface after a 20-h incubation show no linear structures that would be indicative of polymerization. In contrast, a dense and regular distribution of dots of similar size appears, which probably correspond to oligomeric aggregates of denatured monomers (not shown).

In the presence of a PC:SA monolayer but in otherwise identical conditions, the surface was sampled in two different sets of conditions: at mechanical rest, or with a mild stirring of the subphase (see Materials and Methods). The motivation of introducing a mild stirring of the subphase was to perturb the conditions of polymerization, by a hydrodynamic flow. This perturbation will be useful in illustrating and analyzing the differences between the present results and those previously obtained in closely related work (Laliberté and Gicquaud, 1988). Under "stirring" conditions, linear structures clearly appear on the surface, consisting of straight filaments (Fig. 5 *a*), with lengths typically from 1 to 3.5 μm. The thickness of each filament appears to be constant at 6–7 nm, in agreement with the known ultrastructure of F-actin. These filaments are arranged in loose parallel patterns (made up of 5–20 filaments), which clearly contrast with the strong order and close spacing of paracrystalline microfilament sheets made from F-actin solutions (Laliberté and Gicquaud, 1988; Ward et al., 1990; Taylor and Taylor, 1992). Here the word "parallel" does not imply the same polarity of the filaments. In these stirring conditions, isolated filaments are barely seen. Fig. 5 *b* shows the dramatic effect of the lack of stirring of the subphase on actin filament structure, typically observed on samples transferred onto electron microscopic grids after torsion or ellipsometry measurements. The parallel long and straight filaments are no longer present; only single filaments are seen, and these form a continuous 2D network. Another striking feature is the stuctural defects shown by these isolated filaments, such as thickness irregularities and branching points (Fig. 5 *b*). The lengths of these filaments are also shorter: from 0.5 to 1 μm. Nevertheless, these seemingly "abnormal" structures are essentially 1D objects, with an electron density contrast similar to that of straight filaments.

DISCUSSION

The present results show that a nonpolymerizing G-actin solution can be induced to assemble into individual filaments on the surface of a positively charged lipid monolayer. Following initial work (Renault et al., 1997), in this report the combination of ellipsometry, tensiometry, surface rheology, transmission electron microscopy, and dark-field light microscopy is used to investigate this phenomenon and to describe qualitatively and quantitatively some of its kinetic, mechanical, and ultrastructural aspects. Different experimental conditions (G- or F-actin solutions at a bare air/water interface or under a lipid monolayer) are used to evaluate the role of the surface lipids and the dimensionality of the polymerization process, and to kinetically resolve adsorption from rigidification/polymerization.

Purity and reproducibility

The protocols followed for actin purification and manipulation were optimized for an optimal reproducibility of the

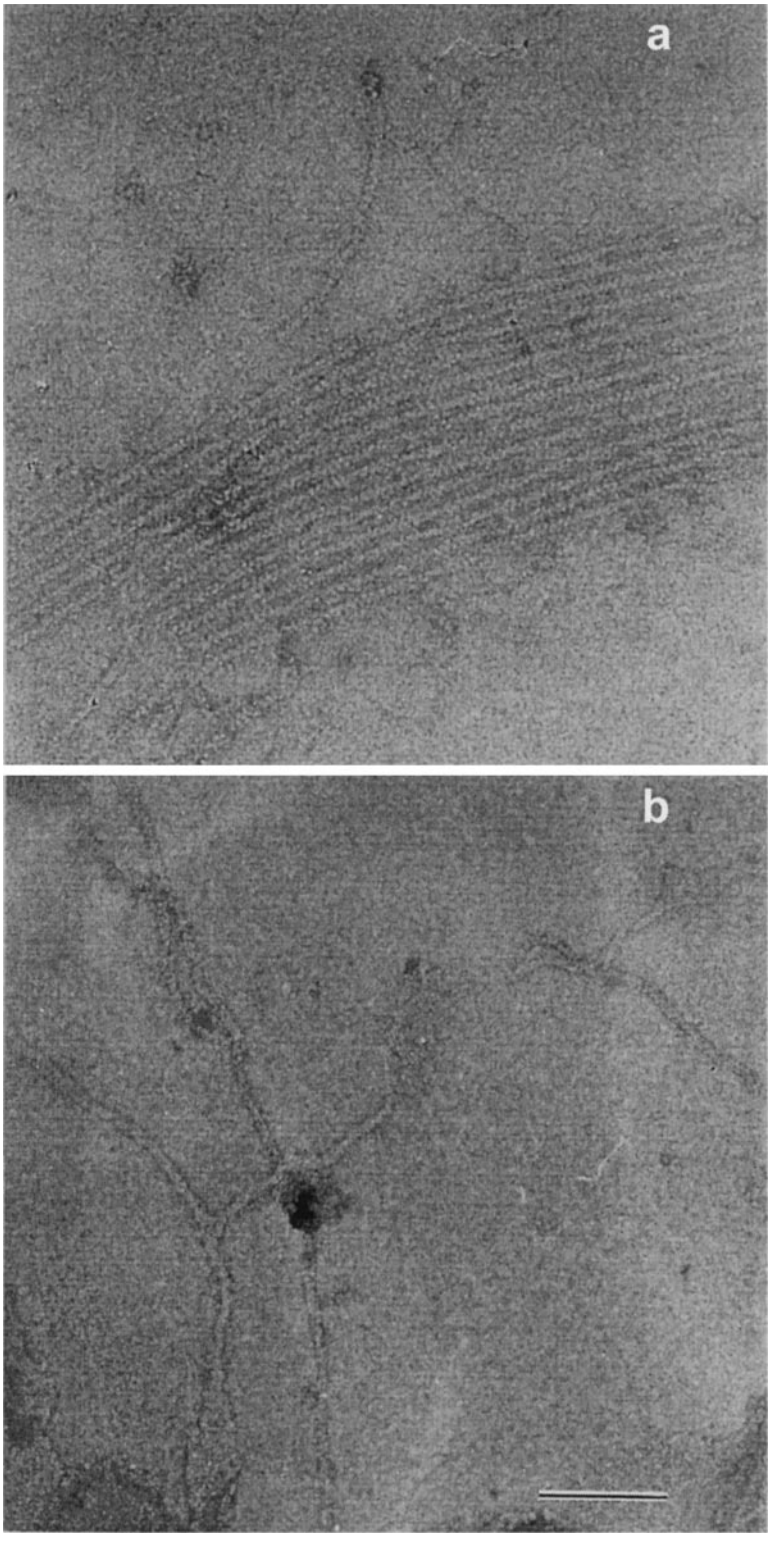

FIGURE 5 Electron microscopy observations of actin on PC:SA monolayers transferred on a carbon grid. Monomeric actin in G-buffer was polymerized at the lipid interface with (*a*) or without (*b*) a mild stirring of the subphase. The bar represents 100 nm.

results: three polymerization/depolymerization cycles with a rapid overnight depolymerization at each step, storage at −80°C, reproducible thawing procedure, and only same-day use of thawed solutions. The solutions used typically had a total concentration of contaminants (larger than 5 kDa) on the order of 0.1–0.2%, as determined by polyacrylamide gel electrophoresis (Fig. 6). In addition, the molecular mass of actin determined by mass spectrometry was within ~50 Da of the expected mass with no apparent proteolysis. In our experience, the usual one-cycle purification procedure gave an insufficient purity (~1% contaminant), which gave fluctuating results in surface rheology experiments. The precautions described above are of critical importance and gave us a satisfactory reproducibility, even

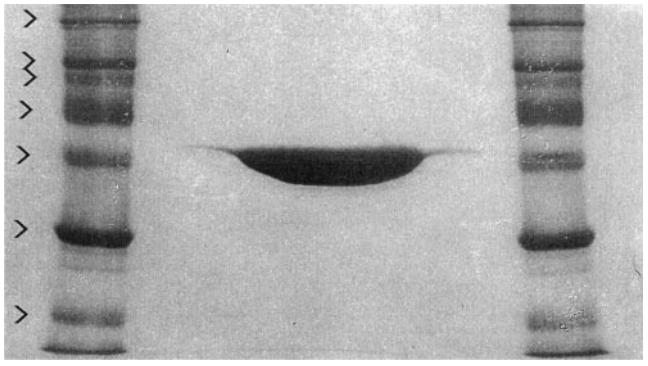

FIGURE 6 Coomassie-stained polyacrylamide gel (10%). Sixty micrograms of actin was loaded, and 4 μg for each of the following molecular mass standards: 21, 31, 45, 66, 97, 116, 200 kDa.

between different purification batches. Ellipsometry results were obtained four to five times, giving very similar results in terms of the angle Δ_{max} and the time constant τ; indeed, the deviation of the fitted quantities between the different experiments was less than the fitting error (see values in Table 1). Shear elastic measurements were made two or three times for each set of conditions, and the kinetic curves gave similar results (see Table 1).

Adsorption kinetics

The ellipsometric angle Δ depends on the refractive index profile perpendicular to the air/water interface. It is analyzed here in a semiquantitative way, by considering it as the sum of two terms: a fixed offset representing the lipid monolayer, and the angle contributed by the proteins in molecular contact with the lipid surface, which reflects the average surface density and thickness of the adsorbed actin layer.

Let us first consider G-actin at the bare air/liquid interface or under the PC:SA monolayer. The short-time monoexponential behavior of the ellipsometric angle Δ (Figs. 1 and 3 *a*) can be accounted for by an effective first-order adsorption process sketched by

$$[\mathrm{A}] \underset{k_-}{\overset{k_+}{\longleftrightarrow}} [\mathrm{B}],$$

where [A] is the volume concentration of actin, [B] is its surface concentration, and k_+ is the on rate, with units of length over time. The equilibrium value [B]/[A] reflects the surface affinity and has units of length. The experimentally observed proportionality between the on rate and the actin concentration (data not shown) is in agreement with this model, as well as the existence of a long time plateau in the ellipsometric angle. One may then ask whether the G-actin adsorption is diffusion limited or not. A simple calculation based on the actin volume concentration, the monomer size ($\sim$5 nm), and the diffusion coefficient of G-actin ($\sim$50 $\mu m^2 s^{-1}$) tells us that the adsorption occurs on a time scale that is within the reaction-limited regime by at least two orders of magnitude. The reaction-limited monoexponential behaviors described for G-actin are also found with F-actin with or without lipids (Figs. 2 *a* and 4 *a*), with slightly larger exponential time constants. Reaction limitation of protein adsorption onto lipids, as opposed to diffusion limitation, has also been observed in other experimental models, such as spectrin or protein 4.1 (Kiernan et al., 1997). It is noteworthy that the presence of lipids slightly reduces the adsorption on rate for both G- and F-actin and leads to a denser and/or thicker surface coverage (Table 1).

After the exponential adsorption phase, in the absence of lipids, the long-time behavior of the ellipsometric signal for both G- and F-actin fits very well with a slow adsorption process with a constant rate that does not saturate (Figs. 1 and 2 *a*). This process is most likely caused by the irreversible denaturation of actin in contact with air. Interestingly, surface denaturation is much slower ($\sim$30 times) with F- than G-actin. In the case of F-actin, the shear rigidity of the interface is not affected in a detectable way by these processes.

The long-time behavior of the G- and F-actin solutions under the PC:SA monolayer are quite different from those in the absence of lipids. Indeed, F-actin under lipids results in an equilibrium situation, with a flat plateau for both the ellipsometric and the rigidity signals (Fig. 4). This suggests that actin filaments are protected from denaturation and build a mechanically stable surface. In contrast to this situation, the lipid interface in contact with a G-actin solution is not stable, but shows a distinctive hyperbolic decrease of the ellipsometric angle. Taken together with the decrease in surface tension, this observation strongly suggests that actin could intercalate into the monolayer, as has been observed in other experimental protein/lipid models (Ellison and Castellino, 1997, and references therein). The hyperbolic variation of the optical signal suggests that the underlying process is a second-order reaction in contrast with the initial exponential adsorption. Moreover, this second-order process occurs on a time scale that is very similar to that of the elasticity increase, thus suggesting a relationship between them.

Surface shear elasticity

Our approach to measuring surface shear elasticity involves a device that applies very small excitation strains (from 10^{-3} down to 10^{-6}). In this range, previous experiments have shown that pure shear elastic response spectra are obtained with 2D protein crystals, and there is a linear stress-strain relationship over the whole range (Vénien-Bryan et al., 1998). This demonstrates that 1) the rotation coupling between the float and the contacting monolayer covered with its underlying structures is satisfactory, and 2) such small strains do not create plastic deformations on fragile surface objects. We currently used strains in the 10^{-4} range, which is very likely to be inside the linear elastic

response domain of surface actin networks. It is noteworthy that surface rheology experiments already reported employed much higher strains in the 0.01–0.05 range (Müller et al., 1991), and that strongly limits the meaning of quantitative comparisons with our work, as explained later.

The following discussion of elasticity focuses on the behavior of G-actin solutions at the PC:SA interface (Fig. 3), and all quantities refer to this experimental situation unless otherwise stated. As previously mentioned, elasticity cannot be measured while the subphase is stirred, so the present discussion only applies to structures obtained in unstirred conditions. Frequency response spectra (data not shown) acquired at different times during the experiments did not show a viscous component, but only an increase in the shear elastic modulus, which was then simply assessed at a fixed rotation frequency of 5 Hz.

Two arguments support the notion that the elasticity increase is entirely due to interfacial structures resulting from the actin-lipid interaction. First, ultrasensitive dark-field video microscopy experiments aimed at visualizing individual filaments over long times revealed filaments "sticking" to the interface without detaching (Fig. 7). In these experiments, no filaments were seen in the bulk solution. Second, the asymptotic value of the elastic modulus is roughly one order of magnitude larger than that for the F-actin solution in the absence of lipids, and the PC:SA monolayer per se has no detectable elasticity—less than 0.1 mN/m. Altogether, these facts suggest that a lipid-actin structure present at the surface is responsible for the observed elasticity.

We must then discuss the nature of these surface structures that increase the surface shear elasticity. Several arguments strongly suggest that actin filaments observed by electron microscopy in unstirred conditions are indeed causing the elasticity increase. In the first place, the analysis of numerous micrographs indicates that filaments form a 2D network that covers most of the surface in a continuous way, with a typical interfilament distance (2D mesh size) of a micron. Is such a network density high enough to account for the elasticity observed at long times? A direct quantitative answer to this question is rather difficult, because the elastic properties of the surface bound polymers seen by electron microscopy are not known. Nevertheless, the 2D mesh size (1 μm) is close to the 3D mesh size of the 25 μg/ml solution when polymerized (2 μm) (Schmidt et al., 1989). In addition, the vertical size of the strained region (5 mm) is four times smaller than its horizontal extension (20 mm). This indicates that the surface elastic modulus of the 2D network (30 mN/m), when corrected for the geometry, is similar to that of the 3D actin solution. This order of magnitude comparison suggests that the surface elasticity of the surface polymerized actin "skin" can indeed be accounted for by the microfilament network seen on the surface. A rigorous comparison of these numbers would require a careful theoretical analysis of the geometry of the strain field, which is simple in 2D but much more complex in the 3D medium. In addition, the actin we used is very pure (0.1–0.2% contaminants in mass), and we did not see any evidence of 2D crystalline arrays of actin by electron microscopy. This is very different from streptavidin crystals formed under a biotinylated lipid monolayer. Indeed, despite the fact that 2D crystals are clearly visible by electron microscopy, they cause an order of magnitude smaller surface shear elasticity, as measured by the same apparatus with an identical geometry (3 mN/m) (Vénien-Bryan et al., 1998). This makes it very unlikely that invisible surface structures contribute to the elasticity. Altogether, these results strongly suggest that the 2D filament network formed at the PC:SA interface over a nonpolymerizing actin solution is indeed the essential cause for the observed increase in surface shear elasticity.

FIGURE 7 Dark-field light microscopy image of a single actin filament (see Materials and Methods). The filament has polymerized from and is attached to a (PC:SA) lipid monolayer supported by a G-actin subphase. The exposure time is 1/25 s, but live video shows a strongly fluctuating shape. The bar represents 10 μm.

The rheology of actin solution has been extensively investigated in bulk (Janmey, 1991; Müller et al., 1991; Wachsstock et al., 1994; Isambert and Maggs, 1996) and at a microscopic scale by the use of microbeads (Ziemann et al., 1994; Amblard et al., 1996; Schnurr et al., 1997; Maggs, 1998). Unfortunately, unlike physical polymer systems, experimental results with actin display a very strong variability. For instance, plateau moduli measured in bulk by different groups are scattered over many orders of magnitude (Maggs, 1997). This comes from some intrinsic features of the actin biochemistry, such as the polydispersity of filament length, from the purity of actin preparations used, and, importantly, from the technical details of rheology experiments. The surface rheology approach described here bears some apparent similarity to an oscillating disk rheometer previously used for measuring the 3D shear elastic modulus of an entangled actin solution (Müller et al., 1991). A typical plateau modulus of 0.1 N/m^2 was found for a 0.1 mg/ml actin solution. Can one make quantitative comparisons between that work and ours? Despite apparent similarities between the two instruments, the set-up of Müller et al. has several important features that make it different from ours: 1) The coupling of the rotating float with the solution

is made by a neutral lipid monolayer of dimyristoylphosphatidylcholine, which is known not to interact with actin (Bouchard et al., 1998). 2) The strain used (~0.05) is roughly three orders of magnitude above our range, and this might affect the linearity of the response. 3) The strain geometries are different in the two instruments, and in particular, the strain in the meniscus region is poorly controlled and probably very high in Müller's work and inadequate for measuring 2D shear elasticity. For all of these reasons, it is not meaningful to look for the length scale that is required for comparing surface and bulk elasticity in the two instruments. Nevertheless, these remarks do not invalidate the above comparison made between our measurements of the elasticity of the 2D and 3D networks, because the same instrument was used.

The kinetics of rigidification follow an exponential behavior, from which the nature of the polymerization kinetics cannot be inferred, because the mechanical effect measured here probably has no simple relationship with the amount of polymer formed at the interface. The exponential elasticity increase is preceded by a 5000-s lag phase, which is longer than the 1800-s adsorption time constant (Fig. 3). This delay between the adsorption and the rigidification has also been observed in the process of 2D crystallization of cholera toxin B, where it was related to the percolation of 2D crystals (Vénien-Bryan et al., 1998). A similar feature was also observed in kinetic analysis of actin polymerization in a suspension of positively charged liposomes in the absence of Mg^{2+} and K^+ ions (Laliberté and Gicquaud, 1988). Here either the surface-induced polymerization has a lag like that of solution polymerization, and/or the elasticity requires the surface concentration of polymer to rise above a critical threshold. The latter interpretation fits well with the general notion that polymer solutions manifest elastic properties only if their concentration is above a threshold where entanglement appears (De Gennes, 1978).

Assembly and microscopic structure of surface-induced actin polymers

Actin polymerization is classically induced in solution by the presence of [KCl] ≈ 50–100 mM and [$MgCl_2$] ≈ 1–2 mM. In the nonpolymerizing conditions used in this work ([KCl] = [$MgCl_2$] = 0), G-Actin is in the Ca^{2+}-bound form and thus has a very limited bulk nucleation rate and a high critical concentration of several hundred micromolar. Because the actin concentration used is 0.6 μM, there is virtually no F-actin in the bulk solution. This is in agreement with results of dark-field light microscopy (Fig. 7 and results to be published). Despite structural and functional differences between Mg^{2+}- and Ca^{2+}-bound forms, Ca^{2+}-bound actin does polymerize in solution, but this polymerization requires KCl and shows a long lag phase (Yasuda et al., 1996; Steinmetz et al., 1997). Actin polymerization in solution is classically thought to require the reduction of the net negative charge of the G-actin monomer by salts (Mg^{2+}, K^+) (Harwell et al., 1980). Here the polymerization of Ca^{2+}-bound actin is obtained despite the absence of KCl. One may thus suggest that surface charges could play a role in reducing the net monomer charge, thus facilitating adsorption and monomer-monomer contacts at the lipid interface. A similar observation has been reported in a bulk assay showing surface-induced polymerization by positively charged liposomes (PC:SA) but not by negatively charged ones (Laliberté and Gicquaud, 1988). Nevertheless, major differences exist between the observations of Laliberté et al. and the present ones. These authors obtained only actin paracrystals, and single filaments were not seen, suggesting that positive liposomes act like high divalent salt concentrations (Harwell et al., 1980). In addition, polymerization with liposomes follows much faster kinetics and does not lead to apparent defects in the helical symmetry. On the contrary, in the present report, only single filaments are observed, with much slower kinetics and with structural defects that will be discussed later. This suggests that lipid surfaces of chemically identical compositions behave differently both quantitatively and qualitatively, when assembled as monolayers or liposome bilayers. A possible cause of this different behavior is that the thermal fluctuations at the scale of the filament length are orders of magnitude smaller in amplitude for a monolayer than for a liposome, because of surface tension. This probably profoundly affects the way monomers and filaments interact with the surface. Other differences, such as the purity of the actin solution, can neither be ruled out nor discussed in the absence of quantitative data on this point in the report mentioned (Laliberté and Gicquaud, 1988). Indeed, these experiments are known to be distressingly sensitive to impurities.

The presence of the PC:SA interface results in the formation of linear actin polymers, whereas only dotlike structures are seen at the bare air/water interface. When the sample is mechanically at rest, the polymers induced by the lipid monolayer present many branching point defects (Fig. 5 *b*). Are these defects induced by the lipid membrane? Interestingly, actin filaments polymerized in classical conditions (i.e., in a homogeneous 3D solution) also display structural defects, such as kinks, spines, and branching points (Steinmetz et al., 1997). These defects are visible 10 min after the onset of polymerization, but they disappear after 30 min, to yield the classical straight helical filaments with constant thickness (Steinmetz et al., 1997). This suggests that G-actin per se, in the absence of a lipid surface, is capable of "misassembly," leading to kinetically favorable monomer-monomer configurations that are metastable and spontaneously disappear in solution. At the lipid interface, similar defect-enriched configurations are apparently stable at long times, except if the subphase is perturbed by a mild stirring. On liposomes, which are not under tension and therefore undergo much larger thermal fluctuations than monolayers, no defects are seen, which suggests that the defects are mechanically fragile but are quenched at rest. Under mechanical stress, provided here by stirring the sub-

phase, or caused by thermal fluctuations on liposomes, defective filaments probably break up to eventually form mechanically stable bona fide actin filaments (Fig. 5 *a*). The process by which defects are produced and quenched at rest might be related to a possible geometric frustration of the helical symmetry of monomer-monomer contacts at the lipid interface. Indeed, this particular symmetry is incompatible with the orientation of actin monomer potentially imposed by actin-lipid interactions. A recent work on hisactophilin-actin interactions at a lipid interface implicitly suggests the possibility of such an electrostatic orientation (Naumann et al., 1996). Further investigations are required to elucidate the nature of the adsorption mechanism and its coupling with polymerization.

The binding of cytosolic proteins to the plasma membrane is often mediated by their attachment to transmembrane proteins, but direct binding to the plasma membrane lipids also occurs and might play an important role in vivo. In the case of actin, experimental in vitro results suggest that several cytosolic proteins could mediate its membrane binding, such as talin, caldesmon, hisactophilin, actinin, or ezrin (Luna and Hitt, 1992; Han et al., 1997; Bretscher et al., 1997; Naumann et al., 1996, and references therein). A study of the actin localization in an epithelial cell line has shown that a pool of nonmonomeric actin is located at the membrane, but nothing indicates a direct interaction rather than an indirect one (Cao et al., 1993). In addition, a report indicates that monomeric actin interacts not only with positive surfaces leading to paracrystals, but also with negative lipid surfaces, despite its net negative charge (Bouchard et al., 1998). In the latter case no paracrystal formation is seen. Because most membrane lipids are neutral or negative, the interaction of actin with negative surfaces is more likely to occur in vivo than the interaction with positive ones. Nevertheless, in vivo evidence for a direct binding of actin to the plasma membrane is missing. In that sense, the present experimental model is not physiological, but it can be helpful for the further study of the physical aspects of molecular assembly on lipid membrane templates in general.

CONCLUSION

The present data demonstrate that a nonpolymerizing G-actin solution can be induced to polymerize into single filaments by and at a positively charged lipid monolayer. The mechanism first involves a monoexponential adsorption process, followed by a marked increase in the surface shear elastic modulus. Actin polymerization essentially occurs at the interface and produces a 2D network of actin filaments, which is probably responsible for the observed elasticity. These observations point toward open questions concerning the detailed molecular mechanism of 2D nucleation and polymerization and its relationship with 3D polymerization. The optical, mechanical, and microscopic imaging methods combined in the present work, together with other tools, should be useful for further studies of protein-lipid interactions and 2D molecular assembly.

We are indebted to Claude Gicquaud for initiating our interest in actin/lipid interactions and for collaborating on the first experiments. We thank Bruno Berge for his constant scientific support. S. Charpak and J. Rossier are acknowlegded for their warm support, E. Beaurepaire for his assistance, and J. P. Le Caer for purity tests using mass spectrometry.

This work was made possible partly by a grant from the Defense Ministry to FA (contract 961177).

REFERENCES

Amblard, F., A. C. Maggs, B. Yurke, A. N. Pargellis, and S. Leibler. 1996. Subdiffusion and anomalous viscoelasticity in actin networks. *Phys. Rev. Lett.* 77:4470–4473.

Berge, B., and A. Renault. 1993. Ellipsometry study of 2D crystallization of 1-alcohol monolayers at the water surface. *Europhys. Lett.* 21: 773–777.

Bouchard, M., C. Paré, J.-P. Dutasta, J.-P. Chauvet, C. Gicquaud, and M. Auger. 1998. Interaction between G-actin and various types of liposomes: a ^{19}F, ^{31}P, and ^{2}H NMR study. *Biochemistry.* 37:3149–3155.

Bretscher, A., D. Reczek, and M. Berryman. 1997. Ezrin: a protein requiring conformational activation to link microfilaments to the plasma membrane in the assembly of cell surface structures. *J. Cell Sci.* 110: 3011–3018.

Cao, L.-G., D. J. Fishkind, and Y.-L. Wang. 1993. Localization and dynamics of nonfilamentous actin in cultured cells. *J. Cell Biol.* 123: 173–181.

Carlier, M.-F. 1991. Actin: protein structure and filament dynamics. *J. Biol. Chem.* 266:1–4.

De Gennes, P. G. 1978. Scaling Concept in Polymer Physics. Cornell University Press, Ithaca, NY.

Ellison, E. H., and F. J. Castellino. 1997. Adsorption of bovine prothrombin to spread phospholipid monolayers. *Biophys. J.* 72:2605–2615.

Grant, N. J., and C. Oriol-Audit. 1983. Supramolecular forms of actin induced by polymamines: an electron microscopy study. *Eur. J. Cell Biol.* 30:67–73.

Haas, H., G. Brezinski, and H. Möhwald. 1995. X-ray diffraction of a protein crystal anchored at the air/water interface. *Biophys. J.* 68: 312–314.

Han, X., G. Li, G. Li, and K. Lin. 1997. Interactions between smooth muscle a-actinin and lipid bilayers. *Biochemistry.* 36:10364–10371.

Harwell, O. D., M. Sweeney, and F. Kirkpatrick. 1980. Conformation changes of actin during formation of filaments and paracrystals and upon interaction with DNAse I, cytochalasin B and phalloidin. *J. Biol. Chem.* 255:1210–1220.

Henderson, R., J. Baldwin, T. Ceska, F. Zemlin, E. Beckmann, and K. Downing. 1990. Model for a structure of bacteriorhodopsin based on hig resolution cryo-electron microscopy. *J. Mol. Biol.* 213:899–929.

Isambert, H., and A. C. Maggs. 1996. Dynamics and rheology of actin solutions. *Macromolecules.* 29:1036–1040.

Jacobson, K., E. D. Sheets, and R. Simson. 1995. Revisiting the fluid mosaic model of membranes. *Science.* 268:1441–1442.

Janmey, P. A. 1991. Physical properties of actin. *Curr. Opin. Cell Biol.* 2:11–17.

Kabsch, W., and J. Vandekerckhove. 1992. Structure and function of actin. *Annu. Rev. Biophys. Biomol. Struct.* 21:49–76.

Kiernan, A. E., R. I. McDonald, R. C. McDonald, and D. Axelrod. 1997. Cytoskeletal protein binding kinetics at planar phospholipid membranes. *Biophys. J.* 73:1987–1998.

Lenne, P.-F. 1998. Deux exemples de cristallisation à la surface de l'eau: cristaux 2D de protéines, et monocouches d'alcools en présence d'amphiphiles solubles. Ph.D. thesis. Université Joseph Fourier, Grenoble, France. 150 pp.

Laliberté, A., and C. Gicquaud. 1988. Polymerization of actin by positively charged liposomes. *J. Cell Biol.* 106:1221–1227.

Luna, E. J., and A. L. Hitt. 1992. Cytoskeleton-plasma membrane interactions. *Science.* 258:955–964.

Maggs, A. C. 1997. Two plateau moduli actin gels. *Phys. Rev. E.* 55: 7396–7400.

Maggs, A. C. 1998. On micro-bead mechanics with actin filaments. *Phys. Rev. E.* 57:2091–2094.

Mannherz, H. G. 1992. Crystallization of actin in complex with actin binding proteins. *J. Biol. Chem.* 267:11661–1164.

Müller, O., H. E. Gaub, M. Barmann, and E. Sackmann. 1991. Viscoelastic moduli of sterically and chemically cross-linked actin networks in the dilute to semi-dilute regime: measurement by an oscillating disk rheometer. *Macromolecules.* 24:3111–3120.

Naumann, C., C. Dietrich, A. Behrisch, T. Bayerl, M. Schleicher, D. Bucknall, and E. Sackmann. 1996. Hisactophilin-mediated binding of actin to lipid lamellae: a neutron reflectivity study of protein membrane coupling. *Biophys. J.* 71:811–823.

Oriol-Audit, C. 1978. Polyamine induced actin polymerization. *Eur. J. Biochem.* 87:371–376.

Pardee, J. D., and J. A. Spudich. 1982. Purification of muscle actin. *Methods Enzymol.* 85:164–181.

Pollard, T. D. 1990. Actin. *Curr. Opin. Cell Biol.* 2:33–40.

Pollard, T. D., S. Almo, S. Quirk, V. Vinson, and E. E. Lattman. 1994. Structure of actin-binding protein: insight about function at atomic resolution. *Annu. Rev. Cell Biol.* 10:207–249.

Renault, A., F. Amblard, C. Gicquaud, and B. Berge. 1997. Actin adsorbed under phospholipid layers. *Eur. Biophys. Conf. Eur. Biophys. J.* 26:119.

Rioux, L., and C. Gicquaud. 1985. Actin paracrystalline sheets formed at the surface of positively charged liposomes. *J. Ultrastruct. Res.* 93: 42–49.

Schmidt, C. F., M. Barmann, G. Isenberg, and E. Sackmann. 1989. Chain dynamics, mesh size, and diffusive transport in networks of polymerized actin. A quasielastic light scattering and microfluorescence light study. *Macromolecules.* 22:3638–3649.

Schnurr, B., F. Gittes, F. C. Macintosh, and C. F. Schmidt. 1997. Determining microscopic viscoelasticity in flexible and semiflexible polymer networks from thermal fluctuations. *Macromolecules.* 30:7781–7792.

Sheterline, P., and J. C. Sparrow. 1994. Biological characteristics of actin. *Protein Profile.* 1:1–12.

Steinmetz, M. O., K. N. Goldie, and U. Aebi. 1997. A correlative analysis of actin filament assembly, structure, and dynamics. *J. Cell Biol.* 138: 559–574.

Taylor, K. E., and D. W. Taylor. 1992. Formation of 2-D paracrystals of F-actin on phospholipid layers mixed with quaternary ammonium surfactants. *J. Struct. Biol.* 108:140–147.

Vénien-Bryan, C., P.-F. Lenne, C. Zakri, A. Renault, A. Brisson, J.-F. Legrand, and B. Berge. 1998. Characterization of the growth of 2D protein crystal on a lipid monolayer by ellipsometry and rigidity measurements coupled to electron microscopy. *Biophys. J.* 74:2649–2657.

Wachsstock, D. H., W. H. Schwarz, and T. D. Pollard. 1994. Cross-linker dynamics determine the mechanical properties of actin gels. *Biophys. J.* 66:801–809.

Ward, R. J., J. F. Menetret, F. Pattus, and K. Leonard. 1990. Method for forming two-dimensional paracrystals of biological filaments on lipid monolayers. *J. Electron Microsc. Tech.* 14:335–341.

Yasuda, R., H. Miyata, and K. Kinosita. 1996. Direct measurement of torsional rigidity of single actin filaments. *J. Mol. Biol.* 263:227–236.

Zakri-Delplanque, C. 1997. Etude de la fusion-crystallisation de monocouches de 1-alcool à la surface de l'eau: mesures d'élasticité latérale par diffraction de rayons X et par une méthode mécanique. Ph.D. thesis, University Joseph Fourier, Grenoble.

Ziemann, F., J. Radler, and E. Sackmann. 1994. Local measurements of viscoelastic moduli of entangled actin networks using an oscillating magnetic bead microrheometer. *Biophys. J.* 66:1–7.